

Five New Monotetrahydrofuran Ring Acetogenins from the Leaves of *Annona muricata*

Lu Zeng, Feng-E Wu, Nicholas H. Oberlies, and Jerry L. McLaughlin*

Purdue University, School of Pharmacy and Pharmacal Sciences, Department of Medicinal Chemistry and Molecular Pharmacology, West Lafayette, Indiana 47907

Soelaksono Sastroridhadjo

Department of Education and Culture, Center of Interuniversities, Biology Division, Bandung Institute of Technology, 10 Ganesha St., Bandung 40132, Indonesia

Received May 10, 1996[®]

Bioactivity-directed fractionation of the leaves of *Annona muricata* resulted in the isolation of annopentocins A (**1**), B (**2**), and C (**3**), and *cis*- and *trans*-annomuricin-D-ones (**4**, **5**). Compounds **1–3** are the first acetogenins reported bearing a mono-tetrahydrofuran (THF) ring with one flanking hydroxyl, on the hydrocarbon side, and another hydroxyl, on the lactone side, that is one carbon away from the THF ring. Compounds **4** and **5** were obtained in a mixture and are new mono-THF ring acetogenins bearing two flanking hydroxyls and an *erythro*-diol located between the THF and the ketolactone rings. Compound **1** was selectively cytotoxic to pancreatic carcinoma cells (PACA-2), and **2** and **3** were selectively cytotoxic to lung carcinoma cells (A-549); the mixture of **4** and **5** was selectively cytotoxic for the lung (A-549), colon (HT-29), and pancreatic (PACA-2) cell lines with potencies equal to or exceeding those of Adriamycin.

Annona muricata L. (Annonaceae), known as “sour sop”, “sir sak”, or “guanabana”, is a popular fruit tree cultivated throughout the tropical regions of the world.¹ The fruit forms the basis of a well-developed juice industry in the tropics, and the seeds are an abundant by-product of this industry.^{2–4} Searching for bioactive components from the seeds previously led us to the isolation of several known mono-tetrahydrofuran (mono-THF) ring acetogenins,^{5–7} the muricatetrocins and gigantetrocins,⁸ muricatacin,⁹ and recently to the new mono-THF ring acetogenins, *cis*-annonacin, *cis*-annonacin-10-one, *cis*-goniothalamycin, arianacin, and javoricin.¹⁰ Parallel work on the leaves has resulted in the isolation of six known compounds,¹¹ gigantetrocin A, annonacin-10-one, muricatetrocins A and B, annonacin, and goniiothalamycin, and twelve new acetogenins, annomuricins A, B,¹¹ and C;¹² muricatocins A, B,¹³ and C;¹² annomutacin,¹⁴ *cis*- and *trans*-10(*R*)-annonacin-A-ones;¹⁴ annohexocin;¹⁵ and murihexocins A and B.¹⁶ Cavé and co-workers previously reported the isolation of four new mono-THF ring acetogenins, murisolin,¹⁷ corossolin, corossolone,¹⁸ and solamin,¹⁹ from the seeds.

So far, more than 230 acetogenins have been found among 26 species of the Annonaceae, and these have been summarized in four review papers.^{20–23} About 90 mono-THF ring acetogenins are classified into six types according to the stereochemistries of the THF rings and their flanking hydroxyls;²³ these are the annonacin, *cis*-annonacin, annonacin A, gigantetrocin A, muricatetrocin A, and muricatacin types of acetogenins.²³ The former three types have a mono-THF ring bearing two flanking hydroxyls, and the latter three types have a mono-THF ring bearing one flanking hydroxyl.

The high potencies of the Annonaceous acetogenins in various bioassay systems have been demonstrated

experimentally to be due to their inhibition of ATP production through both the inhibition of the NADH-ubiquinone oxidoreductase (Complex I) of mitochondrial electron transport systems^{24–28} and the ubiquinone-linked NADH oxidase in the plasma membranes of tumor cells.²⁹ These combined actions may be linked to programmed cell death (apoptosis).³⁰ The acetogenins are effective against drug resistant cell lines, and they are relatively nontoxic to noncancerous cells.^{29,31}

In continuing the fractionation of the extracts of the leaves of *A. muricata*, directed by the brine shrimp lethality test (BST),^{32,33} five new mono-THF ring acetogenins, annopentocins A (**1**), B (**2**), and C (**3**) and *cis*- and *trans*-annomuricin-D-ones (**4**, **5**), have been isolated. Compounds **1–3** (Chart 1) are the first mono-THF ring acetogenins bearing one flanking hydroxyl, on the hydrocarbon side, and another hydroxyl, on the lactone side, that is only one carbon away from the THF ring; these represent a new structural type for the acetogenins. Difference NOE and NOESY experiments, observing the signals around the THF ring in **1–3**, suggested the relative stereochemistries across the THF ring systems, and single-relayed COSY verified that one hydroxyl was separated by a methylene from the THF ring. This new type of acetogenin, namely, the annopentocin A type, exhibited a characteristic ¹H-NMR pattern for the THF ring signals that is distinguishable from all other types of acetogenins.²³ Compounds **4** and **5** were obtained in a mixture and are new mono-THF ring acetogenins bearing two flanking hydroxyls and an *erythro*-diol located between the THF and the ketolactone rings. ¹H-NMR analyses of their Mosher ester derivatives permitted the determinations of the absolute stereochemistries of these compounds.

Compounds **1–5** showed moderate activities in the BST and in a panel of six human solid-tumor cell lines used to evaluate their relative potencies. Compound **1** was selectively cytotoxic to pancreatic carcinoma cells

* To whom correspondence should be addressed. Phone: (317) 494 1455. FAX: (317) 494 6790.

[®] Abstract published in *Advance ACS Abstracts*, October 15, 1996.

Chart 1

	R	R ₁	R ₂	R ₃	R ₄
Annopentocin A (1)	H	H	OH	H	OH
1a	Ac	H	OAc	H	OAc
1b	H	H	O-	H	OCH(CH ₃) ₂ -
1c	TMSi	H	OTMSi	H	OTMSi
1s	(S)-MTPA	H	(S)-OMTPA	H	(S)-OMTPA
1r	(R)-MTPA	H	(R)-OMTPA	H	(R)-OMTPA
Annopentocin B (2)	H	OH	H	OH	H
2a	Ac	OAc	H	OAc	H
2b	H	O-	H	OCH(CH ₃) ₂ -	H
2c	TMSi	OTMSi	H	OTMSi	H
2s	(S)-MTPA	(S)-OMTPA	H	(S)-OMTPA	H
2r	(R)-MTPA	(R)-OMTPA	H	(R)-OMTPA	H
Annopentocin C (3)	H	H (OH)	OH (H)	OH (H)	H (OH)
3a	Ac	H (OAc)	OAc (H)	OAc (H)	H (OAc)
3b	H	H (O-)	O- (H)	OCH(CH ₃) ₂ - (H)	H [OCH(CH ₃) ₂ -]
3c	TMSi	H (OTMSi)	OTMSi (H)	OTMSi (H)	H (OTMSi)
3s	(S)-MTPA	H [(S)-OMTPA]	(S)-OMTPA (H)	(S)-OMTPA (H)	H [(S)-OMTPA]
3r	(R)-MTPA	H [(R)-OMTPA]	(R)-OMTPA (H)	(R)-OMTPA (H)	H [(R)-OMTPA]

Chart 2

	R	R ₁	R ₂
4, 5	H	OH	OH
4b, 5b	H	O-	OCH(CH ₃) ₂ -
4c, 5c	TMSi	OTMSi	OTMSi
4s, 5s	(S)-MTPA	(S)-OMTPA	(S)-OMTPA
4r, 5r	(R)-MTPA	(R)-OMTPA	(R)-OMTPA

(PACA-2), and **2** and **3** were selectively cytotoxic to lung carcinoma cells (A-549). The mixture of **4** and **5** (Chart 2) was the most potent and showed selective activities, comparable to the nonselective potency of Adriamycin, against the lung (A-549), colon (HT-29), and pancreas (PACA-2) cell lines.

Results and Discussion

The NMR, MS, IR, and UV spectral data of compounds **1–3** showed the following features common to the α,β -unsaturated γ -lactone acetogenins with a C-4 hydroxyl group: IR absorptions at ca. 3400 (OH stretch), 1750 cm^{-1} (lactone C=O), and a strong aliphatic C–H absorption below 3000 cm^{-1} ; an absorption maximum (λ_{max}) in the UV spectrum at ca. 215 nm for each compound; and characteristic ¹H- and ¹³C-NMR resonances for H-3/C-3, H-4/C-4, H-33/C-33, H-34/C-34, H-35/C-35, C-1, and C-2;^{20,21} strong absorption in the aliphatic region of the ¹H-NMR spectrum, as well as oxygen-bearing methine resonances in the region ca. δ 3.40–3.90 (see Table 1). EIMS fragment peaks of the TMSi derivatives at m/z 213 confirmed the presence of the α,β -unsaturated γ -lactone, with a C-4 hydroxyl, in all three compounds.³⁴

The molecular weight of each compound was determined by HRFABMS; compounds **1–3** gave respective

MH⁺ values at m/z 613.4685, 613.4699, and 613.4673 corresponding to the formula C₃₅H₆₄O₈+H⁺ (calcd 613.4679). The CIMS of **1–3** exhibited fragments showing successive losses of five m/z 18 (H₂O) units and indicated that there are five hydroxyls in each molecule. This was confirmed by the formation of pentaacetoxy derivatives, **1a–3a**, in which five acetoxy methyl groups were observed in each ¹H-NMR spectrum at δ 2.026–2.084, 2.026–2.083, and 2.026–2.095, respectively (see Table 2).

The ¹H-NMR spectra of **1–3** showed signals at δ 3.90–3.92 and δ 4.18, which corresponded to the ¹³C-NMR signals in the HMQC spectra at δ 82.4 and 80.0 for the 2,5-positions of the substituted THF rings. Only the trilobacin type of acetogenins, which have an adjacent bis-THF ring system bearing two flanking hydroxyls with *threo-trans-erythro-cis-threo* configurations, usually show signals beyond δ 3.95 (two separated multiplet signals at ca. δ 3.95–4.05);³⁵ one 1,3,5-triol moiety in annohexocin shows two proton signals at δ 3.95 and 4.13 (two separated multiplet signals),³⁶ while other types of acetogenins show their proton signals at ca. δ 3.00–3.95.²³ COSY experiments of **1** showed correlations between the signal at δ 3.45 (H-16) to δ 3.91 (H-15), then to δ 1.68 (H-14) and 1.98 (H-14), then to δ 1.56 (H-13) and 2.12 (H-13), and then to δ 4.18 (H-12).

Table 1. NMR Data of **1–3** (in CDCl₃)

position	1		2		3	
	δ_C	$\delta_H J$ (Hz)	δ_C	$\delta_H J$ (Hz)	δ_C	$\delta_H J$ (Hz)
1	174.6		174.6		174.7	
2	131.2		131.2		131.1	
3	33.4	2.40 dddd, 2,2,4,15 2.52 dddd, 2,2,8,15	33.4	2.40 dddd, 2,2,4,15 2.52 dddd, 2,2,8,15	33.4	2.40 dddd, 2,2,4,15 2.52 dddd, 2,2,8,15
4	69.9	3.85 m	69.9	3.85 m	69.9	3.85 m
5	37.4	1.45 m	37.4	1.45 m	37.4	1.45 m
6	25.5	1.25–1.45 m	25.4	1.25–1.45 m	25.5	1.25–1.45 m
7	29.3	1.25–1.45 m	29.3	1.25–1.45 m	29.3	1.25–1.45 m
8	25.7	1.25–1.45 m	25.7	1.25–1.45 m	26.1	1.25–1.45 m
9	37.3	1.45 m	37.3	1.45 m	37.3	1.45 m
10	71.6	3.80 m	71.6	3.80 m	71.7	3.80 m
11	42.4	1.54 m, 1.64 m	42.4	1.54 m, 1.64 m	42.4	1.54 m, 1.65 m
12	80.0	4.18 m	80.0	4.18 m	80.0	4.18 m
13	33.6	1.56 m, 2.12 m	33.7	1.56 m, 2.12 m	33.2	1.57 m, 2.12 m
14	27.9	1.68 m, 1.98 m	27.8	1.68 m, 1.98 m	27.9	1.68 m, 1.98 m
15	82.4	3.91 q 7	82.4	3.90 q 7	82.4	3.92 q 7
16	73.9	3.45 m	73.9	3.47 m	73.8	3.48 m
17	30.0	1.56 m	30.4	1.56 m	30.1	1.52 m
18	29.7	1.60 m	30.1	1.60 m	29.8	1.55 m
19	74.3	3.42 m	74.3	3.41 m	74.6	3.58 m
20	74.5	3.42 m	74.6	3.41 m	74.8	3.62 m
21	33.1	1.45 m	33.1	1.45 m	31.8	1.42 m
22	25.3	1.29 m	25.7	1.29 m	25.3	1.29 m
23–29	29.4–29.7	1.20–1.35 m	29.4–29.7	1.20–1.35 m	29.4–29.7	1.20–1.35 m
30	31.9	1.31 m	31.9	1.31 m	31.9	1.31 m
31	22.7	1.26 m	22.7	1.26 m	22.7	1.26 m
32	14.1	0.88 t 7	14.1	0.88 t 7	14.1	0.88 t 7
33	78.2	5.07 dq 2, 7	78.2	5.07 dq 2, 7	78.2	5.07 dq 2, 7
34	152.3	7.12 q 2	152.3	7.12 q 2	152.3	7.12 q 2
35	19.0	1.43 d 7	19.0	1.43 d 7	19.0	1.43 d 7

Table 2. ¹H-NMR Data of **1a–3a** and **1b–3b** (in CDCl₃)

position	1a	1b	2a	2b	3a	3b
	$\delta_H J$ (Hz)	$\delta_H J$ (Hz)	$\delta_H J$ (Hz)	$\delta_H J$ (Hz)	$\delta_H J$ (Hz)	$\delta_H J$ (Hz)
3	2.51 dddd, 2,2,5,15 2.56 dddd, 2,2,8,15	2.40 dddd, 2,2,4,15 2.52 dddd, 2,2,8,15	2.51 dddd, 2,2,5,15 2.56 dddd, 2,2,8,15	2.40 dddd, 2,2,4,15 2.52 dddd, 2,2,8,15	2.51 dddd, 2,2,5,15 2.56 dddd, 2,2,8,15	2.40 dddd, 2,2,4,15 2.52 dddd, 2,2,8,15
4	5.10 dddd, 5,5,8,8	3.85 m	5.10 dddd, 5,5,8,8	3.85 m	5.10 dddd, 5,5,8,8	3.85 m
5	1.40 m	1.45 m	1.40 m	1.45 m	1.45 m	1.45 m
6	1.25–1.45 m	1.25–1.45 m	1.25–1.45 m	1.25–1.45 m	1.25–1.45 m	1.25–1.45 m
7	1.25–1.45 m	1.25–1.45 m	1.25–1.45 m	1.25–1.45 m	1.25–1.45 m	1.25–1.45 m
8	1.25–1.45 m m	1.25–1.45 m m	1.25–1.45 m m	1.25–1.45 m m	1.25–1.45 m m	1.25–1.45 m m
9	1.45 m	1.46 m	1.45 m	1.45 m	1.50 m	1.45 m
10	4.93 m	3.81 m	4.94 m	3.80 m	4.93 m	3.80 m
11	1.56 m, 1.88 m	1.40 m, 1.54 m	1.54 m, 1.88 m	1.40 m, 1.54 m	1.56 m, 1.88 m	1.54 m, 1.65 m
12	3.92 m	4.19 m	3.92 m	4.19 m	3.93 m	4.18 m
13	1.46 m, 2.06 m	1.54 m, 2.12 m	1.56 m, 2.12 m	1.58 m, 2.14 m	1.46 m, 2.06 m	1.58 m, 2.13 m
14	1.54 m, 1.94 m	1.73 m, 1.97 m	1.68 m, 1.98 m	1.68 m, 1.98 m	1.56 m, 1.95 m	1.71 m, 1.98 m
15	3.95 q 6	3.90 q 7	3.96 q 7	3.92 q 7	3.97 q 7	3.90 td 7, 8
16	4.85 q 6	3.45 ddd 3, 7, 9	4.80 m	3.47 q 7	4.82 m	3.43 m
17	1.52 m, 1.58 m	1.60 m	1.55 m	1.60 m	1.52 m, 1.58 m	1.40 m
18	1.45–1.57 m	1.50 m	1.45–1.57 m	1.50 m	1.45–1.57 m	1.50 m, 1.70 m
19	4.97 m	3.58 m	4.96 m	3.58 m	4.94 m	3.99 m
20	5.01 m	3.60 m	4.97 m	3.60 m	4.95 m	4.03 m
21	1.45–1.57 m	1.50 m	1.45–1.47 m	1.50 m	1.45–1.57	1.40 m, 1.52 m
22	1.29 m	1.28 m	1.29 m	1.28 m	1.20–1.35 m	1.29 m
23–29	1.20–1.35 m	1.20–1.35 m	1.20–1.35 m	1.20–1.35 m	1.20–1.35 m	1.20–1.35 m
30	1.31 m	1.31 m	1.31 m	1.31 m	1.31 m	1.31 m
31	1.26 m	1.26 m	1.26 m	1.26 m	1.26 m	1.26 m
32	0.88 t 7	0.88 t 7	0.88 t 7	0.88 t 7	0.88 t 7	0.88 t 7
33	5.02 dq 2, 7	5.07 dq 2, 7	5.02 dq 2, 7	5.07 dq 2, 7	5.02 dq 2, 7	5.07 dq 2, 7
34	7.08 q 2	7.12 q 2	7.08 q 2	7.12 q 2	7.08 q 2	7.12 q 2
35	1.40 d 7	1.43 d 7	1.40 d 7	1.43 d 7	1.40 d 7	1.43 d 7
Me		1.37 s, 1.37 s		1.37 s, 1.37 s		1.33 s, 1.43 s
AcO	2.026 s, 2.033 s, 2.076 s, 2.082 s, 2.084 s		2.026 s, 2.033 s, 2.074 s, 2.078 s, 2.083 s		2.026 s, 2.032 s, 2.041 s, 2.047 s, 2.095 s	

These protons were related to carbons at δ 73.9 (C-16), 82.4 (C-15), 27.9 (C-14), 33.6 (C-13), and 80.0 (C-12). All these ¹³C-NMR signals closely resembled those of mono-THF ring acetogenins bearing one flanking hydroxyl, but all of these proton signals were shifted downfield. Double-relayed COSY of **1** also showed a

correlation between δ 3.91 (H-15) and δ 4.18 (H-12), which confirmed the relationship of the 2,5-protons of the substituted THF ring. The configuration of the THF ring and the flanking hydroxyl were considered to be *threo* because the chemical shift of the hydroxylmethine proton appeared at δ 3.45 (H-16), which matched the

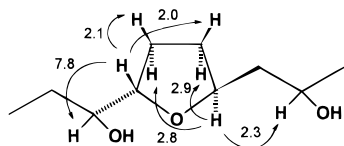


Figure 1. Difference NOE experiments on **1** (numbers on the arrows indicate the NOE enhancements by percentage).

range of similar proton signals among the acetogenins.^{20–23}

With the contiguous carbon skeletons of **1–3** determined, the elucidation of further relative and absolute stereochemistries remained to be ascertained. Such relative configurations are usually determined by a straightforward comparison of the NMR shifts of the naturally occurring compounds with those of synthetic model mono-THF analogues.^{36,37} Because **1–3** represent a new structural type, however, their NMR data did not match any of the model compounds. The relative stereochemistries of the THF rings in **1–3** were thus determined here by a series of difference NOE and NOESY experiments. As illustrated in Figure 1, which shows **1** as an example, when the proton at δ 4.18 (H-12) was irradiated, the protons at δ 2.12 (H-13 α), 1.68 (H-14 α), and 3.80 (H-10) showed enhancements of 2.9, 2.8, and 2.3%, while, when the proton at δ 3.91 (H-15) was irradiated, the protons at δ 1.98 (H-14 β), 1.56 (H-13 β), and 3.45 (H-16) showed enhancements of 2.1, 2.0, and 7.8%. Also in NOESY experiments, the correlations among protons at δ 4.18 (H-12) and 2.12 (H-13 α), 1.68 (H-14 α), and 3.80 (H-10), and protons at δ 3.91 (H-15) and 1.98 (H-14 β), 1.56 (H-13 β), and 3.45 (H-16) were observed. These NOE experiments established that the relative stereochemistry of the THF ring in **1** is of the *trans* configuration. Similar NMR data of **2** and **3** permitted us to conclude that **1–3** all have the same *trans*-THF ring systems.

The presence of 1,2-diols in **1–3** was proven by the formation of the respective acetonide derivative (**1b–3b**). The acetyl methyl groups in **1** and **2** appeared at δ 1.37 as one singlet, while in **3**, they appeared at δ 1.33 and 1.43 as two singlets; these data demonstrated that the 1,2-diols in **1** and **2** have *threo* configurations, and in **3** the 1,2-diol has the *erythro* configuration.³⁸ The placement of the hydroxyl groups at the proper distance from the THF rings was made first by single- and double-relayed COSY experiments. In the single-relayed COSY spectra of **1–3**, correlations between the

protons at δ 3.80 (H-10) and 4.18 (H-12) were observed and showed that two protons have a four-bond relationship. In the double-relayed COSY spectrum of **3**, a correlation between the signals at δ 3.58 (H-19) and 3.48 (H-16) was observed, and, in the COSY spectra of the acetonide derivatives (**1b** and **2b**), correlations between δ 3.58 (H-19) and 3.45 (H-16) (in **1b**) and between δ 3.58 (H-19) and 3.47 (H-16) (in **2b**) were observed and established a five bond relationship for these protons (Figure 2).

All of these relative placements of the hydroxyl groups and the THF rings were then confirmed by EIMS fragmentations (Figure 3) and HREIMS on critical fragments. In **1**, one hydroxyl can be placed at C-10, which showed a fragment at m/z 385.2226 ($C_{19}H_{37}O_4Si_2$, calcd for 385.2230); one hydroxyl at C-16, which showed a fragment at m/z 469.2811 ($C_{24}H_{45}O_5Si_2$, calcd for 469.2806); and the 1,2-diol at C-19 and C-20, which showed fragments at m/z 271.2460 ($C_{16}H_{35}OSi$, calcd for 271.2457) and m/z 710.4135 (for $C_{34}H_{69}O_7Si_4$, calcd for 701.4120). Thus, the THF ring can be placed at C-12. The same peaks were observed in **2** and **3** only with slight differences in intensities (Figure 3).

The stereochemistries at C-4, C-10, and C-16 in **1–3** were determined by Mosher ester methods.^{39–41} The different signs of (*S*)- and (*R*)-MTPA esters (Table 3) permitted us to conclude that C-4, C-10, and C-16 have (*R*), (*R*), and (*S*) configurations, respectively. The stereochemistries of the 1,2-diols in **1** and **2** were determined by observing the ¹H-NMR pattern of the acetonide derivatives (**1b** and **2b**), in which **1b** exhibited a pattern of a doublet of double doublets for H-16 at δ 3.45 in this 1,2,5-triol moiety, while **2b** showed a quartet pattern for H-16 at δ 3.47 in the 1,2,5-triol moiety.^{8,16} These different patterns indicated that **1** has an (*R,R*)-diol and **2** has an (*S,S*)-diol. The absolute stereochemistries of the 1,2-diol in **3** remain unsolved because the MTPA data of critical protons could not be differentiated. Thus, the structures of **1–3** are determined as illustrated.

Compounds **4** and **5** were obtained as a mixture in the ratio of ca. 1:1. Their molecular formulas were determined by HRFABMS, which gave m/z 613.4667 ($C_{35}H_{64}O_8+H^+$, calcd for 613.4679). NMR, MS, IR, and UV spectral data of **4** and **5** showed the following characteristic features of the ketolactone moiety in place of the α,β -unsaturated γ -lactone group with a C-4 hydroxyl as in **1–3**: IR absorption at 1765 cm^{-1} (lactone

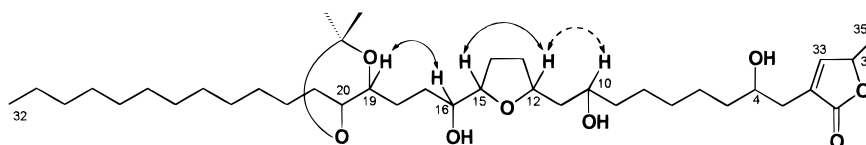


Figure 2. Single- and double-relayed COSY experiments of **1b** and **2b** (dotted and solid arrows show single- and double-relayed correlations, respectively).

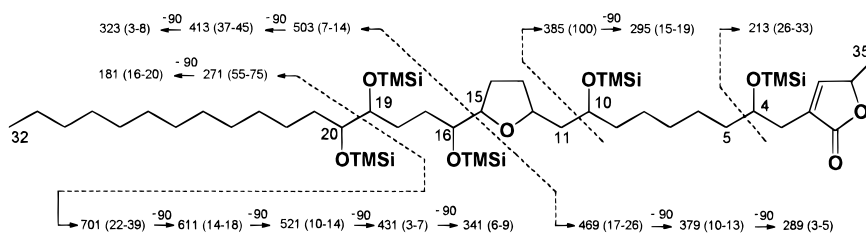


Figure 3. Mass spectral fragmentations (m/z) of **1c–3c** (the range of peak intensities are indicated in parentheses).

Table 3. Characteristic $^1\text{H-NMR}$ Data of Mosher Esters of **1s–3s** and **1r–3r** for Determination of Stereochemistry

position	1s δ_{H}	1r δ_{H}	$\Delta\delta_{1\text{s}-1\text{r}}$	2s δ_{H}	2r δ_{H}	$\Delta\delta_{2\text{s}-2\text{r}}$	3s δ_{H}	3r δ_{H}	$\Delta\delta_{3\text{s}-3\text{r}}$
35	1.26	1.29	-0.03	1.26	1.30	-0.04	1.26	1.30	-0.04
34	4.83	4.89	-0.06	4.83	4.88	-0.05	4.83	4.88	-0.05
33	6.70	6.90	-0.20	6.70	6.90	-0.20	6.70	6.90	-0.20
1									
2									
3	2.49	2.56	-0.07	2.50	2.57	-0.07	2.50	2.57	-0.07
	2.41	2.43	-0.02	2.40	2.43	-0.03	2.40	2.43	-0.03
4	5.15	5.24	<i>R</i>	5.17	5.25	<i>R</i>	5.17	5.25	<i>R</i>
5	1.54	1.52	+0.02	1.53	1.51	+0.02	1.53	1.51	+0.02
10	5.15–5.20	5.15–5.20	<i>R</i>	5.15–5.20	5.15–5.20	<i>R</i>	5.15–5.20	5.15–5.20	<i>R</i>
11	1.56	1.60	-0.04	1.54	1.59	-0.05	1.55	1.59	-0.04
12	3.83	3.82	+0.01	3.86	3.85	+0.01	3.87	3.85	+0.02
13	1.94	1.86	+0.08	1.92	1.85	+0.07	1.94	1.86	+0.08
	1.41	1.39	+0.02	1.39	1.36	+0.03	1.41	1.38	+0.03
14	1.90	1.87	+0.03	1.88	1.85	+0.03	1.89	1.86	+0.03
	1.43	1.40	+0.03	1.43	1.40	+0.03	1.41	1.39	+0.02
15	3.90	3.88	+0.02	3.89	3.88	+0.01	3.89	3.88	+0.01
16	4.81	4.84	<i>S</i>	4.84	4.86	<i>S</i>	4.85	4.86	<i>S</i>
17	1.27	1.30	-0.03	1.28	1.31	-0.03	1.29	1.32	-0.03
19	5.04	5.19		5.03	5.11		5.10–5.15	5.11–5.16	
20	4.98	5.15		5.03	5.19		5.13–5.20	5.14–5.22	

C=O) and 1715 cm^{-1} (C=O); an absorption maximum (λ max) in the UV spectrum at 205 nm; and characteristic $^1\text{H-}$ and $^{13}\text{C-NMR}$ resonances for H-2, H-3, H-4, H-35, C-1, C-4, and C-34 (Table 4).^{20,21} The successive losses of four H_2O molecules (m/z 18) in their EIMS and hydroxylated carbon signals at δ 73.9, 74.3, 74.4, and 74.5 in their $^{13}\text{C-NMR}$ spectra revealed the presence of four hydroxyl groups. Two of these hydroxyl groups were proven to be an *erythro* 1,2-diol by the formation of acetone derivatives (**4b** and **5b**) in which two separated acetyl methyl signals at δ 1.33 and 1.43 were observed.³⁸ The other two hydroxyl groups were considered to be the flanking hydroxyls of the THF ring, because $^1\text{H-}$ and $^{13}\text{C-NMR}$ data demonstrated the characteristic features of a mono-THF ring bearing two flanking hydroxyls; namely, the features of the annonacin type of acetogenins.²³ Also, the comparison of these NMR data with those of synthetic model compounds permitted us to determine that the THF ring and the flanking hydroxyls have *threo-trans-threo* configurations.^{36,37}

The placements of the hydroxyls and the THF ring were made by observing the EIMS fragmentations of TMSi derivatives (**4c** and **5c**) (Figure 4). HREIMS of the fragments of m/z 313.1839 (calcd 313.1835 for $\text{C}_{16}\text{H}_{29}\text{O}_4\text{Si}$), m/z 559.3321 (calcd 559.3306 for $\text{C}_{27}\text{H}_{55}\text{O}_6\text{Si}_3$), and m/z 271.2466 (calcd 271.2457 for $\text{C}_{16}\text{H}_{35}\text{OSi}$) placed the hydroxyls at C-10, C-11, C-15, and C-20 and the THF ring at C-16/C-19, respectively. The stereochemistries of the two ring flanking hydroxyls were both determined by the Mosher ester method to be of (*R*) configuration;^{39–41} thus, the 2,5-positions of the substituted THF ring were of the (*R,R*) forms, respectively. The stereochemistries at C-4 in **4** and **5** were

deduced to be (*R*) based on the hypothesis that the ketolactone acetogenins are all derived from the 4-OH γ -lactone acetogenins which all possess C-4(*R*) configurations. The stereochemistries of the remaining C-10 and C-11 chiral positions cannot be solved by the Mosher ester method because the MTPA groups interfere with each other. Compounds **4** and **5** were named *cis*- and *trans*-annonuricin-D-ones, relating their parent acetogenin, annonuricin D, to the closely related series of annonuricins A–C.^{11,12}

Table 5 summarizes the bioactivities of compounds **1–5**. All of the compounds showed significant activities in the BST and in a panel of six human solid tumor cell lines; the mixture of **4** and **5** was the most active with selectivities toward the lung (A-549), colon (HT-29), and pancreas (PACA-2) cell lines that were equal to or greater than the potency of Adriamycin.^{42–47} Compound **1** was selectively cytotoxic to the pancreatic carcinoma cell line (PACA-2), and **2** and **3** were selectively cytotoxic to the lung carcinoma cell line (A-549). Comparison of the moderate cytotoxicity values of these single-ring compounds with those of other types of acetogenins shows that the bis-THF ring compounds are more potent than non-adjacent bis-THF ring compounds, which themselves are more potent than the mono-THF ring compounds, which, in turn, are more potent than non-ring compounds.^{20–23}

Experimental Section

General Experimental Procedures. Optical rotation determinations were made on a Perkin-Elmer 241 polarimeter. FTIR spectra were obtained on a Perkin-Elmer 1420. $^1\text{H-NMR}$ (500 MHz), difference NOE, 2-D

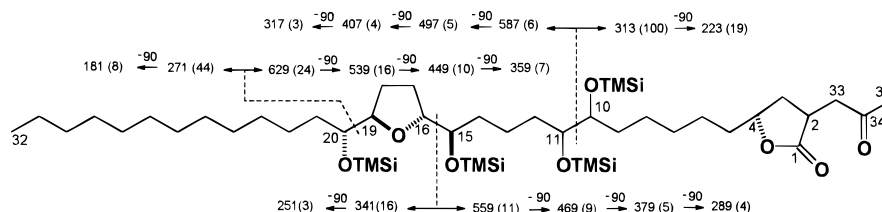
**Figure 4.** Mass spectral fragmentations (m/z) of **4c** and **5c** (the range of peak intensities are indicated in parentheses).

Table 4. ¹H-NMR Data of **4**, **5**, **4b**, **5b**, **4s**, **5s**, **4r**, and **5r** (CDCl₃)

position	4, 5 ^a (δ _C)	4 [δ _H J(Hz)]	5 [δ _H J(Hz)]	4b [δ _H J(Hz)]	5b [δ _H J(Hz)]	4s, 5s (δ _H)	4r, 5r (δ _H)	Δδ _{4s-4r/5s-5r}
1	178.2, 178.3							
2	34.4, 36.6	3.04 m	3.02 m	3.04 m	3.02 m			
3	33.4, 35.3	2.60 m 1.50 m	2.24 m 1.98 m	2.60 m 1.50 m	2.24 m 1.98 m			
4	78.9, 79.3	4.39 dddd 11.5, 7.5, 5.5, 5.0	4.55 dddd 8.5, 9.0, 5.5, 2.5	4.39 dddd 11.5, 7.5, 5.5, 5.0	4.55 dddd 8.5, 9.0, 5.5, 2.5			
5	35.1, 35.5	1.75 m, 1.48 m	1.68 m, 1.54 m	1.75 m, 1.48 m	1.68 m, 1.54 m			
6	25.5, 25.6	1.22–1.80 m	1.22–1.80 m	1.22–1.80 m	1.22–1.80 m			
7	29.3	1.22–1.80 m	1.22–1.80 m	1.22–1.80 m	1.22–1.80 m			
8	25.7	1.22–1.80 m	1.22–1.80 m	1.22–1.80 m	1.22–1.80 m			
9	37.3	1.44–1.46 m	1.44–1.46 m	1.44–1.48 m	1.44–1.48 m			
10	73.9	3.45 m	3.45 m	4.01 m	4.01 m			
11	74.3	3.45 m	3.45 m	4.01 m	4.01 m			
12	33.6	1.44–1.46 m	1.44–1.46 m	1.44–1.48 m	1.44–1.48 m			
13	22.7	1.22–1.80 m	1.22–1.80 m	1.22–1.80 m	1.22–1.80 m			
14	35.0	1.44–1.46 m	1.44–1.46 m	1.44–1.46 m	1.44–1.46 m	1.55	1.59	+0.04
15	74.4	3.41 m	3.41 m	3.40 m	3.40 m	5.03	4.96	R
16	82.5	3.80 m	3.80 m	3.80 m	3.80 m	4.01	3.92	-0.09
17	28.7	1.66 m, 1.98 m	1.66 m, 1.98 m	1.67 m, 1.99 m	1.67 m, 1.99 m	1.55, 1.93	1.38, 1.66	-0.17, -0.27
18	28.7	1.66 m, 1.98 m	1.66 m, 1.98 m	1.67 m, 1.99 m	1.67 m, 1.99 m	1.55, 1.93	1.38, 1.66	-0.17, -0.27
19	82.7	3.80 m	3.80 m	3.80 m	3.80 m	4.01	3.92	-0.09
20	74.5	3.41 m	3.41 m	3.40 m	3.40 m	5.03	4.96	R
21	33.2	1.44–1.46 m	1.44–1.46 m	1.44–1.46 m	1.44–1.46 m	1.55	1.59	+0.04
22	25.9	2.61 dd 18.5, 8.5	2.61 dd 18.5, 9.5	2.61 dd 18.5, 8.5	2.61 dd 18.5, 9.5			
23–29	29.4–29.7	1.22–1.80 m	1.22–1.80 m	1.22–1.80 m	1.22–1.80 m			
30	31.9	1.22–1.80 m	1.22–1.80 m	1.22–1.80 m	1.22–1.80 m			
31	22.7	1.26 m	1.26 m	1.26 m	1.26 m			
32	14.1	0.88 t 7	0.88 t 7	0.88 t 7	0.88 t 7			
33	44.2, 44.8	2.61 m	2.67 dd 18.5, 9	2.61 m	2.67 dd 18.5, 9			
34	205.4, 205.5	3.11 dd 18.5, 3.5	3.04 dd 18.5, 3.5	3.11 dd 18.5, 3.5	3.04 dd 18.5, 3.5			
35	29.8, 29.9	2.20 s	2.20 s	2.20	2.20 s			
Me				1.33 s, 1.43 s	1.33 s, 1.43 s			

^a The assignments were made by DEPT and HMQC.

Table 5. Bioactivities of **1–5** from *Annona muricata*

compound	BST ^a	A-549 ^b	MCF-7 ^c	HT-29 ^d	A-498 ^e	PC-3 ^f	PACA-2 ^g
1	8.9	1.71 × 10 ⁻¹	17.93	1.63	6.07 × 10 ⁻¹	1.14	3.58 × 10 ⁻²
2	11.2	2.74 × 10 ⁻²	3.56	1.64	3.79 × 10 ⁻¹	2.12 × 10 ⁻¹	1.62 × 10 ⁻¹
3	13.8	2.06 × 10 ⁻²	2.97	1.24	2.58 × 10 ⁻¹	2.28 × 10 ⁻¹	4.28 × 10 ⁻¹
4,5	4.8	<10 ⁻²	6.11 × 10 ⁻¹	<10 ⁻²	1.22 × 10 ⁻¹	1.32	<10 ⁻²
Adriamycin ^h	2.57 × 10 ⁻¹	4.28 × 10 ⁻³	4.95 × 10 ⁻¹	4.98 × 10 ⁻²	4.62 × 10 ⁻²	5.83 × 10 ⁻²	4.23 × 10 ⁻³

^a Brine shrimp lethality test (LC₅₀ ppm).^{32,33} ^b Human lung carcinoma (ED₅₀ μg/mL).⁴² ^c Human breast carcinoma.⁴³ ^d Human colon adenocarcinoma.⁴⁴ ^e Human renal carcinoma.⁴² ^f Human prostate adenocarcinoma.⁴⁵ ^g Human pancreatic carcinoma.⁴⁶ ^h Positive control; brine shrimp LC₅₀ taken from Ratnayake *et al.*⁴⁷

COSY, NOESY, and HMQC spectra, referenced to TMS unless otherwise stated, and ¹³C-NMR (125 MHz) spectra referenced to and in CDCl₃, were obtained on a Varian VXR-500S. LREIMS and CIMS were obtained on a Finnigan 4000. LREIMS of TMSi derivatives and all high resolution MS were obtained by peak matching, with perfluorokerosene used as an internal standard, on a Kratos MS50.

In all column chromatography, the extracts were first adsorbed onto Si gel before loading onto the open column. Si gel 60, 60–200 mesh (Selecto brand), purchased in bulk through Fisher Scientific, was used for open columns. Baker flash column Si gel, 40 μm diameter, was used for flash-column chromatography. Amberlite XAD-2 nonionic polymeric adsorbents were purchased from Aldrich Chemical, Inc., and were washed with MeOH, CHCl₃, and hexane before using. The solvents used for extraction and partitions, as well as for chromatography, were reagent grade. TLC plates were visualized by spraying with 5% phosphomolybdic acid followed by heating. Rainin HPXL pumps and a Rainin Model UV-1 ultraviolet detector, controlled by Dynamax version 1.2 software, were used in all HPLC isolations. Normal-phase, analytical, and preparatory

HPLC runs were performed using Rainin columns packed with Dynamax-60A 8-μm Si gel. Reversed-phase HPLC was performed on Rainin 21.4 × 250 mm i.d. columns packed with Dynamax-60A 8 μm C₁₈.

Plant Material. The leaves (2.0 kg) of *Annona muricata* L. were obtained from fruit-producing trees growing in the experimental orchard of Bandung Institute of Technology and were dried and pulverized through an 8-mm sieve in an electric mill.

Biological Evaluations. The extracts, fractions, and isolated compounds were routinely tested for toxicity in the BST.^{32,33} Crude extracts resulting in LC₅₀ values of less than 250 ppm or pure compounds with LC₅₀ values of less than 40 ppm were considered significantly active. Cytotoxicity to human solid-tumor cells was evaluated at the Purdue Cell Culture Laboratory, Purdue Cancer Center, using standard protocols for A-549 lung carcinoma,⁴² MCF-7 breast carcinoma,⁴³ HT-29 colon adenocarcinoma,⁴⁴ A-498 kidney carcinoma,⁴² PC-3 prostate adenocarcinoma,⁴⁵ and PACA-2 pancreatic carcinoma⁴⁶ cell lines. Generally, cytotoxicity ED₅₀ values less than 20 μg/mL for crude extracts and less than 4 μg/mL for pure compounds were considered active.

Extraction and Isolation. The leaves (2.0 kg) were percolated by 95% EtOH to give 386 g of an extract (F001, BST LC₅₀ 30.5 ppm). The EtOH extract was partitioned between CH₂Cl₂ and H₂O (1:1). The H₂O-soluble fraction (F002) was freeze-dried to yield a sticky yellow mass (260 g), while the CH₂Cl₂-soluble fraction was concentrated by rotary evaporation to yield a residue of 126 g (F003, BST LC₅₀ 19.6 ppm). F003 was then partitioned between 90% aqueous MeOH and hexane (1:1). The two phases were dried by rotary evaporation to yield the hexane-soluble fraction (F006 BST LC₅₀ >100 ppm) (11 g) and an aqueous MeOH-soluble fraction (F005, BST LC₅₀ 1.6 ppm) (115 g).

Open column chromatography of F005 (55 g) was performed on 250 g of Amberlite XAD-2 resin eluted by hexane, hexane–Me₂CO (1:1), and then Me₂CO. Flash column chromatography of the hexane–Me₂CO (1:1) residue (10.2 g, BST LC₅₀ 0.98 ppm) from the Amberlite column, with 0–25% MeOH in CH₂Cl₂, eluted over Baker 40 μm Si gel, separated mixtures of active compounds from inert materials as determined by the BST. Active fractions were pooled by activity and subjected to repeated chromatography, by open columns and flash columns over Si gel, in two solvent systems using gradients of CH₂Cl₂–EtOAc or gradients of hexane–Me₂CO. Impure components were combined according to their similar appearance on tlc analysis, and these were again subjected to elution on open columns and flash columns using the two solvent systems as described above. From these impure fractions, the five new compounds were isolated by normal- and reversed-phase HPLC. The Rainin Dynamax-60A 8-μm silica support eluted with 3–15% MeOH–THF (9:1) in hexane was used for normal-phase HPLC separations, and the Rainin Dynamax-60A 8-μm C₁₈ support eluted with 30% H₂O in MeCN was used for reversed-phase HPLC separations to give the new acetogenins, annopentocins A (**1**), B (**2**), and C (**3**) (8, 10, and 7 mg, respectively), and the mixture of *cis*- and *trans*-annomuricin-D-ones (**4**) and (**5**) (12 mg).

TMSi Derivatives of 1–5. Samples of less than 1 mg were dried *in vacuo* in the presence of P₂O₅ and KOH as drying agents. The dry sample was reacted with 20 μL of *N,O*-bis-(trimethylsilyl)-acetamide (BSA). The reaction mixture was heated at 70 °C for 30 min to yield the trimethylsilyl (TMSi) ethers that were analyzed by EIMS.

MTPA Derivatives of 1–5. To an acetogenin (0.5–1 mg, in 0.5 mL of CH₂Cl₂) were sequentially added pyridine (0.1 mL), 4-(dimethylamino)pyridine (0.1 mg), and 15 mg of (*R*)-(-)- α -methoxy- α -(trifluoromethyl)-phenylacetyl chloride. The mixture was stirred at room temperature from 4 h to overnight and passed through a disposable pipet (0.6 × 4 cm) containing Si gel (60–200 mesh) and eluted with 3 mL of CH₂Cl₂. The CH₂Cl₂ residue, dried *in vacuo*, was redissolved in CH₂Cl₂ and washed in 1% NaHCO₃ (5 mL) and H₂O (2 × 5 mL); the CH₂Cl₂ layer was dried *in vacuo* to give the (*S*)-Mosher esters. The use of (*S*)-(+)- α -methoxy- α -(trifluoromethyl)-phenylacetyl chloride gave the (*R*)-Mosher esters. Both yields were typically higher than 90%.

Annopentocin A (1): white, amorphous powder, [α]_D²⁵ 12° (*c* 14, CHCl₃); UV (MeOH) λ max (ϵ) 215 nm, (9,600); IR ν max 3395 (OH), 2930 and 2855 (CH), 1745

(C=O, lactone), 1470 cm⁻¹ (CH); ¹H-NMR data (500 MHz, CDCl₃), see Table 1; ¹³C-NMR data (125 MHz, CDCl₃), see Table 1; CIMS *m/z* MH⁺ 613 (14), with 5 × H₂O losses at 595 (45), 577 (28), 559 (20), 541 (13), and 523 (6); HRFABMS *m/z* 613.4685 (calcd for C₃₅H₆₄O₈ + H, 613.4679); (*R*)-Mosher pentaester of **1** (**1s**), ¹H-NMR data (500 MHz, CDCl₃), see Table 3; (*S*)-Mosher pentaester of **1** (**1r**), ¹H-NMR data (500 MHz, CDCl₃), see Table 3; acetate derivative of **1** (**1a**), ¹H-NMR data (500 MHz, CDCl₃), see Table 2; acetonide derivative of **1** (**1b**), ¹H-NMR data (500 MHz, CDCl₃), see Table 2; TMSi derivative of **1** (**1c**), see Figure 2.

Annopentocin B (2): white oil, [α]_D²⁵ 15° (*c* 10, CHCl₃); UV (MeOH) λ max (ϵ) 214 nm, (9,800); IR ν max 3400 (OH), 2935 and 2845 (CH), 1749 (C=O, lactone), 1465 cm⁻¹ (CH); ¹H-NMR data (500 MHz, CDCl₃), see Table 1; ¹³C-NMR data (125 MHz, CDCl₃), see Table 1; CIMS *m/z* MH⁺ 613 (19), with 5 × H₂O losses at 595 (57), 577 (44), 559 (38), 541 (22), and 523 (10); HRFABMS *m/z* 613.4699 (calcd for C₃₅H₆₄O₈ + H, 613.4679); (*R*)-Mosher pentaester of **2** (**2s**), ¹H-NMR data (500 MHz, CDCl₃), see Table 3; (*S*)-Mosher pentaester of **2** (**2r**), ¹H-NMR data (500 MHz, CDCl₃), see Table 3; acetate derivative of **2** (**2a**), ¹H-NMR data (500 MHz, CDCl₃), see Table 2; acetonide derivative of **2** (**2b**), ¹H-NMR data (500 MHz, CDCl₃), see Table 2; TMSi derivative of **2** (**2c**), see Figure 2.

Annopentocin C (3): white oil, [α]_D²⁵ 9° (*c* 11, CHCl₃); UV (MeOH) λ max (ϵ) 214 nm, (9,750); IR ν max 3410 (OH), 2930 and 2835 (CH), 1741 (C=O, lactone), 1455 cm⁻¹ (CH); ¹H-NMR data (500 MHz, CDCl₃), see Table 1; ¹³C-NMR data (125 MHz, CDCl₃), see Table 1; CIMS *m/z* MH⁺ 613 (29) with 5 × H₂O losses at 595 (65), 577 (49), 559 (39), 541 (31), and 523 (19); HRFABMS *m/z* 613.4673 (calcd for C₃₅H₆₄O₈ + H, 613.4679); (*R*)-Mosher pentaester of **3** (**3s**), ¹H-NMR data (500 MHz, CDCl₃), see Table 3; (*S*)-Mosher pentaester of **3** (**3r**), ¹H-NMR data (500 MHz, CDCl₃), see Table 3; acetate derivative of **3** (**3a**), ¹H-NMR data (500 MHz, CDCl₃), see Table 2; acetonide derivative of **3** (**3b**), ¹H-NMR data (500 MHz, CDCl₃), see Table 2; TMSi derivative of **3** (**3c**), see Figure 2.

***cis*- and *trans*-Annomuricin-D-ones (4, 5):** white powder, [α]_D²⁵ 15° (*c* 10, CHCl₃); UV (MeOH) λ max (ϵ) 205 nm, (7,750); IR ν max 3425 (OH), 2925 and 2835 (CH), 1765 (C=O, lactone), 1715 (C=O), 1455 and 1367 (CH); ¹H-NMR data (500 MHz, CDCl₃), see Table 4; ¹³C-NMR data (125 MHz, CDCl₃), see Table 4; CIMS *m/z* MH⁺ 613 (31) with 4 × H₂O losses at 595 (82), 577 (37), 559 (25), and 541 (17); HRFABMS *m/z* 613.4667 (calcd for C₃₅H₆₄O₈+H, 613.4679); (*R*)-Mosher tetraester of **4**, **5** (**4s**, **5s**), ¹H-NMR data (500 MHz, CDCl₃), see Table 4; (*S*)-Mosher tetraester of **4**, **5** (**4r**, **5r**), ¹H-NMR data (500 MHz, CDCl₃), see Table 4; acetonide derivative of **4**, **5** (**4b**, **5b**), ¹H-NMR data (500 MHz, CDCl₃), see Table 2; TMSi derivative of **4**, **5** (**4c**, **5c**), see Figure 4.

Acknowledgment. This investigation was supported by R01 grant CA30909 from the National Cancer Institute, National Institutes of Health, and a stipend to F. E. W. from the K. C. Wang Education Foundation, Hong Kong, and a fellowship to N. H. O. from the Purdue Research Foundation. We are also grateful to the Cell Culture Laboratory, Purdue Cancer Center, for fruitful discussions concerning the cytotoxicity data.

References and Notes

- (1) Morton, J. *Fruits of Warm Climates*; Media Inc.: Miami, FL, 1973; pp 75–80.
- (2) Awan, J. A.; Kar, A.; Udoudoh, P. J. *Plant Foods Human Nut.* **1980**, *30*, 163–168.
- (3) Kooiman, P. *Carbohydr. Res.* **1971**, *20*, 329–337.
- (4) Koesriharti, In *Plant Resources of South-East Asia, No. 2, Edible Fruits and Nuts*; Verheij, E. W., Coronel, R. E., Eds.; Pudoc Wageningen, Prosea Foundation: Bogor, Indonesia, and Pudoc-DLO: S Wageningen, Netherlands, 1991; pp 75–78.
- (5) Rieser, M. J.; Fang, X.-P.; Rupprecht, J. K.; Hui, Y.-H.; Smith, D. L.; McLaughlin, J. L. *Planta Med.* **1993**, *59*, 91–92.
- (6) McCloud, T. G.; Smith, D. L.; Chang, C.-J.; Cassady, J. M. *Experientia* **1987**, *43*, 947–949.
- (7) Xu, L.-Z.; Chang, C.-J.; Yu, J.-G.; Cassady, J. M. *J. Org. Chem.* **1989**, *4*, 5418–5421.
- (8) Rieser, M. J.; Fang, X.-P.; Anderson, J. E.; Miesbauer, L.; Smith, D. L.; McLaughlin, J. L. *Helv. Chim. Acta* **1993**, *76*, 2433–2444, and erratum **1994**, *77*, 882.
- (9) Rieser, M. J.; Kozlowski, J. F.; Wood, K. V.; McLaughlin, J. L. *Tetrahedron Lett.* **1991**, *32*, 1137–1140.
- (10) Rieser, M. J.; Gu, Z.-M.; Fang, X.-P.; Zeng, L.; Wood, K. V.; McLaughlin, J. L. *J. Nat. Prod.* **1996**, *59*, 100–108.
- (11) Wu, F.-E.; Gu, Z.-M.; Zeng, L.; Zhao, G.-X.; Zhang, Y.; McLaughlin, J. L.; Sastrodihardjo, S. *J. Nat. Prod.* **1995**, *58*, 830–836.
- (12) Wu, F.-E.; Zeng, L.; Gu, Z.-M.; Zhao, G.-X.; Zhang, Y.; Schwedler, J. T.; McLaughlin, J. L.; Sastrodihardjo, S. *J. Nat. Prod.* **1995**, *58*, 909–915.
- (13) Wu, F.-E.; Gu, Z.-M.; Zeng, L.; Zhao, G.-X.; Zhang, Y.; Schwedler, J. T.; McLaughlin, J. L.; Sastrodihardjo, S. *J. Nat. Prod.* **1995**, *58*, 902–908.
- (14) Wu, F.-E.; Zhao, G.-X.; Zeng, L.; Zhang, Y.; Schwedler, J. T.; McLaughlin, J. L.; Sastrodihardjo, S. *J. Nat. Prod.* **1995**, *58*, 1430–1437.
- (15) Zeng, L.; Wu, F.-E.; McLaughlin, J. L. *Bioorg. Med. Chem. Lett.* **1995**, *5*, 1865–1868.
- (16) Zeng, L.; Wu, F.-E.; Gu, Z.-M.; McLaughlin, J. L. *Tetrahedron Lett.* **1995**, *36*, 5291–5294.
- (17) Myint, S. H.; Laurens, A.; Hocquemiller, R.; Cavé, A. *Heterocycles* **1990**, *31*, 861–867.
- (18) Cortes, D.; Myint, S. H.; Laurens, A.; Hocquemiller, R.; Leboeuf, M.; M. Cavé, M. *Can. J. Chem.* **1991**, *69*, 8–11.
- (19) Myint, S. H.; Cortes, D.; Laurens, A.; Hocquemiller, R.; Leboeuf, M.; Cavé, A.; Cotte, J.; Queros, A. M. *Phytochemistry* **1991**, *30*, 3335–3338.
- (20) Rupprecht, J. K.; Hui, Y.-H.; McLaughlin, J. L. *J. Nat. Prod.* **1990**, *53*, 237–278.
- (21) Fang, X.-P.; Rieser, M. J.; Gu, Z.-M.; Zhao, G.-X.; McLaughlin, J. L. *Phytochem. Anal.* **1993**, *4*, 27–48 and 49–67.
- (22) Gu, Z.-M.; Zhao, G.-X.; Oberlies, N. H.; Zeng, L.; McLaughlin, J. L. *Recent Advances in Phytochemistry*; Arnason, J. T., Mata, R., Romeo, J. T., Eds.; Plenum Press: New York, 1995; Vol. 29, pp 249–310.
- (23) Zeng, L.; Ye, Q.; Oberlies, N. H.; Shi, G.; Gu, Z.-M.; McLaughlin, J. L. *Nat. Prod. Rep.* **1996**, *13*, 275–306.
- (24) Londershausen, M.; Leicht, W.; Lieb, F.; Moeschler, H.; Weiss, H. *Pestic. Sci.* **1991**, *33*, 427–438.
- (25) Ahammadsahib, K. I.; Hollingworth, R. M.; McGovren, P. J.; Hui, Y.-H.; McLaughlin, J. L. *Life Sci.* **1993**, *53*, 1113–1120.
- (26) Lewis, M. A.; Arnason, J. T.; Philogene, B. J. R.; Rupprecht, J. K.; McLaughlin, J. L. *Pestic. Biochem. Physiol.* **1993**, *45*, 15–23.
- (27) Esposti, M. D.; Ghelli, A.; Ratta, M.; Cortes, D. *Biochem. J.* **1994**, *301*, 161–167.
- (28) Hollingworth, R. M.; Ahammadsahib, K. I.; Gadelhak, G.; McLaughlin, J. L. *Biochem. Soc. Trans.* **1994**, *22*, 230–233.
- (29) Morre, D. J.; de Cabo, R.; Farley, C.; Oberlies, N. H.; McLaughlin, J. L. *Life Sci.* **1995**, *56*, 343–348.
- (30) Wolvetang, E. J.; Johnson, K. L.; Krauer, K.; Ralph, S. J.; Linnane, A. W. *FEBS Lett.* **1994**, *339*, 40–44.
- (31) Oberlies, N. H.; Jones, J. L.; Corbett, T. H.; Fotopoulos, S. S.; McLaughlin, J. L. *Cancer Lett.* **1995**, *96*, 55–58.
- (32) Meyer, B. N.; Ferrigni, N. R.; Putnam, J. E.; Jacobson, L. B.; Nichols, D. E.; McLaughlin, J. L. *Planta Med.* **1982**, *45*, 31–34.
- (33) McLaughlin, J. L. *Methods in Plant Biochemistry, Vol. 6*; Hostettman, K. Ed.; Academic Press: London, 1991; pp 1–30.
- (34) Rupprecht, J. K.; Chang, C.-J.; Cassady, J. M.; McLaughlin, J. L.; Mikolajczak, K. L.; Weisleder, D. *Heterocycles* **1986**, *24*, 1197–1201.
- (35) Zhao, G.-X.; Gu, Z.-M.; Zeng, L.; Chao, J. F.; Kozlowski, J. F.; Wood, K. V.; McLaughlin, J. L. *Tetrahedron* **1995**, *26*, 7149–7160.
- (36) Harmange, J. C.; Figadere, B.; Cave, A. *Tetrahedron Lett.* **1992**, *33*, 5749–5752.
- (37) Fujimoto, Y.; Murasaki, C.; Shimada, H.; Nishioka, S.; Kakinuma, K.; Singh, S.; Singh, M.; Gupta, Y. K.; Sahai, M. *Chem. Pharm. Bull.* **1994**, *42*, 1175–1184.
- (38) Gu, Z.-M.; Fang, X.-P.; Zeng, L.; Kozlowski, J. F.; McLaughlin, J. L. *Bioorg. Med. Chem. Lett.* **1994**, *4*, 473–478.
- (39) Dale, J. A.; Mosher, H. S. *J. Am. Chem. Soc.* **1973**, *95*, 512–519.
- (40) Ohtani, I.; Kusumi, T.; Kashman, Y.; Kakisawa, H. *J. Am. Chem. Soc.* **1991**, *113*, 4092–4096.
- (41) Rieser, M. J.; Hui, Y.-H.; Rupprecht, J. K.; Kozlowski, J. F.; Wood, K. V.; McLaughlin, J. L.; Hanson, P. R.; Zhuang, Z.; Hoye, T. R. *J. Am. Chem. Soc.* **1992**, *114*, 10 203–10 213.
- (42) Giard, D. J.; Aaronson, S. A.; Todaro, G. J.; Arnstein, P.; Kersey, J. H.; Dosik, H.; Parks, W. P. *J. Natl. Cancer Inst.* **1973**, *51*, 1417–1423.
- (43) Soule, H. D.; Vazquez, J.; Long, A.; Albert, S.; Brennan, M. J. *Natl. Cancer Inst.* **1973**, *51*, 1409–1416.
- (44) Fogh, J.; Trempe, G. In *Human Tumor Cells*; Fogh, J. Ed.; Plenum Press: New York, 1975; pp 115–159.
- (45) Kaighn, M. E.; Narayan, K. S.; Ohnuki, Y.; Lechner, J. F.; Jones, L. W. *Invest. Urol.* **1979**, *17*, 16–23.
- (46) Yunis, A. A.; Arimura, G. K.; Russin, D. *Int. J. Cancer* **1977**, *19*, 128–135.
- (47) Ratnayake, S.; Gu, Z.-M.; Miesbauer, L. R.; Smith, D. L.; Wood, K. V.; Evert, D. R.; McLaughlin, J. L. *Can. J. Chem.* **1994**, *72*, 287–293.

NP960447E